Propofol-induced HOXA11-AS promotes proliferation, migration and invasion, but inhibits apoptosis in hepatocellular carcinoma cells by targeting miR-4458

FURONG SONG[1,2], JUN LIU[1], YAWEI FENG[1] and YI JIN[2]

Departments of [1]Anesthesiology and [2]Pathology, The Third Affiliated Hospital of Sun Yat-Sen University, Guangzhou, Guangdong 510630, P.R. China

Received September 25, 2019; Accepted June 3, 2020

DOI: 10.3892/ijmm.2020.4667

Abstract. Propofol is a commonly used drug for the induction and maintenance of anesthesia. Previous studies have reported that propofol is involved in the progression of numerous human cancer types, including hepatocellular carcinoma (HCC). However, the underlying molecular mechanisms in HCC are yet to be elucidated. The present study aimed to investigate the potential mechanism of propofol in HCC development. MTT assay, flow cytometry analysis and Transwell assays were conducted to examine cell proliferation, apoptosis, migration and invasion, respectively. Western blotting was also performed to determine the protein expression levels of Bcl-2 and cleaved-caspase 3. An *in vivo* experiment was performed to assess the effect of propofol on tumor growth. Moreover, reverse transcription-quantitative PCR was conducted to measure the mRNA expression levels of HOMEOBOX A11 (HOXA11) antisense RNA (HOXA11-AS) and microRNA (miR)-4458. Dual-luciferase reporter and RNA pull-down assays were performed to evaluate the target relationship between HOXA11-AS and miR-4458. It was demonstrated that propofol inhibited HCC cell proliferation, migration and invasion, and promoted cell apoptosis *in vitro*. Furthermore, propofol could suppress tumor growth *in vivo*. Propofol suppressed the expression of HOXA11-AS in HCC cells, while HOXA11-AS overexpression reversed the inhibitory effect of propofol treatment on cell progression in HCC. In addition, miR-4458 was identified as a target of HOXA11-AS, and miR-4458 inhibition reversed the effect of HOXA11-AS knockdown on HCC cell progression. The results also indicated that propofol promoted the expression of miR-4458, while HOXA11-AS restored this effect in HCC. Thus, it was suggested that propofol suppressed cell progression by modulating the HOXA11-AS/miR-4458 axis in HCC.

Correspondence to: Dr Yi Jin, Department of Pathology, The Third Affiliated Hospital of Sun Yat-Sen University, 600 Tianhe Road, Guangzhou, Guangdong 510630, P.R. China
E-mail: song15812412574@163.com

Key words: propofol, hepatocellular carcinoma, HOMEOBOX A11 antisense RNA, microRNA-4458

Introduction

As a type of primary liver cancer, hepatocellular carcinoma (HCC) has a high mortality rate with 782,000 deaths annually worldwide (1-3). Although significant progress has been achieved in HCC treatment, the overall prognosis is still not optimal due to the high metastasis rate and high recurrence rate (4,5). For patients with HCC, surgical resection is the most effective treatment method (6). It has been reported that anesthetics can affect the treatment of multiple human cancer types, such as osteosarcoma (7), ovarian cancer (8) and breast cancer (9). Therefore, it is important to investigate the underlying mechanism of action of anesthetics affecting the development of cancer.

Propofol is a short-acting intravenous anesthetic that is widely used to relieve the pain of patients during surgery (10). Previous studies have revealed that propofol is associated with the progression of numerous human tumors. For instance, Zhang *et al* (11) revealed that propofol induced cell proliferation and invasion, but restrained cell apoptosis in gallbladder cancer. Moreover, Wang *et al* (12) showed that propofol suppressed cell proliferation and metastasis in glioma, while Liu *et al* (13) reported that propofol served a tumor suppression role in pancreatic cancer. In addition, Ou *et al* (14) demonstrated that propofol repressed HCC cell proliferation and metastasis, as well as induced apoptosis. These findings suggest that propofol serves different roles in human cancer types. However, the exact function and mechanism of propofol in HCC requires further investigation.

As a family of non-coding transcripts that are >200 nucleotides in length, long non-coding RNAs (lncRNAs) participate in various biological processes, such as differentiation, cell development, survival and apoptosis (15,16). Previous studies have reported that lncRNAs, such as antisense noncoding RNA in the INK4 locus (17), taurine upregulated 1 (18) and DiGeorge syndrome critical region gene 5 (19), could be dysregulated by propofol treatment in human cancer types. Moreover, multiple lncRNAs have been demonstrated to serve vital roles in HCC. For example, MYD88 innate

immune signal transduction adaptor can promote HCC cell proliferation and metastasis (20). Furthermore, E74-like ETS transcription factor 209 could suppress tumor progression via inhibiting cell metastasis in HCC (21). HOMEOBOX A11 (HOXA11) antisense RNA (HOXA11-AS) has also been identified to be associated with HCC (22). However, the regulatory mechanism of HOXA11-AS in HCC is not fully characterized, and whether there is an association between propofol and HOXA11-AS is yet to be elucidated.

MicroRNAs (miRNAs/miRs), a family of endogenous RNAs with 19-22 nucleotides, have crucial roles in human cancer, including HCC (23). In recent decades, numerous miRNAs have been identified to be involved in the promotion of HCC. For example, Wang *et al* (24) identified that miR-194-5p repressed HCC cell proliferation and induced cell apoptosis. Moreover, Kabir *et al* (25) reported that miR-7 affected cell viability and metastasis in HCC. miR-4458 has also been shown to exert an anti-tumor effect in HCC (26). Thus, as lncRNAs can regulate miRNA expression levels and activities by sponging to miRNAs (27), whether HOXA11-AS can target miR-4458 in HCC requires further investigation.

The present study aimed to evaluate the functions of propofol in tumor progression in HCC. In addition, the influences of propofol on HOXA11-AS and miR-4458 were investigated, as well as the roles of HOXA11-AS and miR-4458 in HCC cell proliferation, apoptosis and metastasis.

Materials and methods

Cell culture. HCC cell lines Hep3B (cat. no. SCSP-5045) and Huh-7 (cat. no. SCSP-526) were purchased from the Type Culture Collection of the Chinese Academy of Sciences. HCC cells were cultured in DMEM (cat. no. 10099-141; Gibco; Thermo Fisher Scientific, Inc.) supplemented with 10% FBS (cat. no. 12483-012; Gibco; Thermo Fisher Scientific, Inc.) and 1% penicillin/streptomycin (cat. no. 15140-122; Gibco; Thermo Fisher Scientific, Inc.) in an incubator at 37˚C with 5% CO_2.

Propofol treatment. Propofol (cat. no. BP1031 MSDS; Sigma-Aldrich; Merck KGaA) was dissolved in DMSO (40 mg/ml; cat. no. D8371; Beijing Solarbio Science & Technology Co., Ltd.) and diluted in the culture medium at 37˚C for 15 min to achieve final concentrations of 2.5, 5 and 10 μg/ml for the experiments. Then, HCC cells were exposed to different concentrations of propofol (2.5, 5 or 10 μg/ml) at 37˚C for 24 h according to previous studies (28,29). The control groups were treated with equal volume of 0.2% DMSO (500 μl; cat. no. D8371; Beijing Solarbio Science & Technology Co., Ltd.) at 37˚C for 24 h.

Cell transfection. The overexpression plasmid of HOXA11-AS and corresponding empty plasmid of pcDNA 3.1 (Vector); small interfering RNA targeting HOXA11-AS (si-HOXA11-AS#1, 5'-CTACCATCCCTGAGCCTTA-3'; si-HOXA11-AS#2, 5'-CAGAAGAATGGTACAATCCAAG-3'; si-HOXA11-AS#3, 5'-AGGATGAGATTCAGAATATGAAG-3') and its matched negative control (si-NC; 5'-CCTATCTGGTCAACACGTATT-3'); mimics of miR-4458 (miR-4458; 5'-AGAGGUAGGUGUGGAAGAA-3') and its corresponding NC (miR-NC; 5'-UUCUCCGAACGUGUCACGUUU-3'); inhibitors of miR-4458 (anti-miR-4458; 5'-UUCUUCCACACCUACCUCU-3') and its NC (anti-miR-NC; 5'-CAGUACUUUUGUGUAGUACAA-3') were all purchased from Sangon Biotech Co., Ltd.

Hep3B and Huh-7 cells were seeded into 6-well plates at a density of $2.0x10^4$ cells/well and transfected with 50 nM synthetic oligonucleotides or vectors using Lipofectamine® 2000 (cat. no. 11668-109; Invitrogen; Thermo Fisher Scientific, Inc.). After HCC cells were transfected for 12 h and transfection efficiencies were measured (Fig. S1), cells were treated with 5 μg/ml propofol for 24 h at 37˚C.

MTT assay. Cell proliferation was determined using a MTT assay. Hep3B and Huh-7 cells were seeded into 96-well plates at a density of $1x10^3$ cells/well and incubated overnight. After the aforementioned transfection and treatment, 20 μl MTT (5 mg/ml; cat. no. M1020; Beijing Solarbio Science & Technology Co., Ltd.) was added into each well at 24, 48 and 72 h, and then further incubated at 37˚C for an additional 4 h, followed by centrifugation at 37˚C for 10 min at a speed of 1,000 x g. Subsequently, the supernatant was discarded and 150 μl DMSO was added to dissolve the formazan crystals. The optical density (OD) value at 570 nm was measured via a microplate reader (BioTek Instruments, Inc.).

Flow cytometry analysis. The apoptosis of HCC cells was assessed via an Annexin V- FITC/propidium iodide (PI) Apoptosis Detection kit (cat. no. A211-01/02; Vazyme Biotech Co., Ltd.). After relevant transfection and treatment, HCC cells were harvested and resuspended at a concentration of $1.0x10^6$ cells/ml. Then, 5 μl AnnexinV-FITC and 5 μl PI were added into the cell suspension to the stain of cells. After 15 min of incubation in the dark at room temperature, the number of apoptotic cells was analyzed within 1 h via a flow cytometry (FACSCalibur; BD Biosciences) with software FlowJo 7.6.1 (FlowJo LLC). The number of apoptotic cells was the sum of the early apoptosis number (the lower right quadrant) and the late apoptosis number (the upper right quadrant).

Western blotting. After relevant transfection and treatment, Hep3B and Huh-7 cells were harvested and lysed in RIPA buffer (cat. no. R0010; Beijing Solarbio Science & Technology Co., Ltd.) containing protease inhibitor (cat. no. P8340 MSDS; Sigma-Aldrich; Merck KGaA) and phosphatase inhibitor (cat. no. P2745 MSDS; Sigma-Aldrich; Merck KGaA) to isolate total protein. Then, a bicinchoninic acid protein quantification kit (cat. no. E112-01/02; Vazyme Biotech Co., Ltd.) was used to examine the concentration of proteins. Next, a total of 50 μg proteins were separated by 10% SDS-PAGE (cat. no. P1200; Beijing Solarbio Science & Technology Co., Ltd.) and transferred onto PVDF membranes (cat. no. PVM020C-160; Pall Corporation). The membranes were blocked with 5% non-fat milk for 2 h at room temperature and then incubated with primary antibodies against Bcl-2 (cat. no. ab182858; 1:2,000; Abcam), cleaved-caspase 3 (c-caspase 3; cat. no. ab2302; 1:2,000; Abcam), proliferating cell nuclear antigen (PCNA; cat. no. ab152114; 1:2,000; Abcam), cyclinD1 (cat. no. ab190564; 1:5,000; Abcam), C-Myc (cat. no. Ab39688; 1:1,000; Abcam), Bax (cat. no. ab59348;

1:1,000; Abcam), c-poly(ADP-ribose) polymerase 1 (PARP; cat. no. ab4380; 1:1,000; Abcam), E-cadherin (cat. no. ab76055; 1:1,000; Abcam), N-cadherin (cat. no. ab18203; 1:1,000; Abcam), Vimentin (cat. no. ab45939; 1:1,000; Abcam) or GAPDH (cat. no. ab8245; 1:5,000; Abcam) overnight at 4˚C. Subsequently, the membranes were probed with corresponding horseradish peroxidase (HRP)-conjugated secondary antibody (cat. no. ab150117; 1:5,000; Abcam) for 1 h at room temperature. The protein bands were determined using an enhanced chemiluminescence reagent (cat. no. E411-03/04/05; Vazyme Biotech Co., Ltd.) and analyzed using the software ImageJ v1.8.0 (National Institutes of Health).

Transwell assay. Following relevant transfection and treatment, HCC cells were collected. For the detection of cell migration, collected HCC cells were suspended in medium without serum and 500 μl cell suspension ($5.0x10^5$ cells/ml) was seeded into the upper chamber of a 24-well Transwell (cat. no. 3379; 8 μm; Corning, Inc.). The bottom chamber was plated with 600 μl DMEM with 10% FBS. After 24 h of incubation at 37˚C, cells that remained on the upper chamber were removed using a cotton swab and cells that migrated were fixed with 90% methanol for 30 min at 37˚C and stained with 0.1% crystal violet for 15 min at 37˚C (cat. no. IC0600; Beijing Solarbio Science & Technology Co., Ltd.). The migrated cells were counted under a light microscope at x100 magnification.

For the detection of cell invasion, the upper chamber was coated with Matrigel (cat. no. 356234; Beijing Solarbio Science & Technology Co., Ltd.) for 30 min at 37˚C and the other procedures were the same as aforementioned. The numbers of migrated and invaded cells were represented by the average number of cells in five randomly selected fields.

In vivo experiment. The suspension of Hep3B cells ($1x10^6$ cells) was subcutaneously injected into the right leg near the abdomen of BALB/c nude mice (n=12; Shanghai SLAC Laboratory Animal Co., Ltd.; age, 5 weeks; sex, female; weight, 19-21 g). The mice were housed under pathogen-free conditions with a 12-h light/dark cycle at 27˚C and 45% humidity and fed sterile fodder and drinking water. All inoculations were performed under anesthesia with isoflurane. The parameters of anesthesia were monitored as follows: i) Ocular reflex, nystagmus indicated if the anesthesia was too shallow, the pupil dilated during anesthesia excitement period and the would pupil dilate excessively if the anesthesia was excessive; ii) eyelid reflex, when the medial or lateral canthus was touched, the mice blinked and this reflex disappeared during surgical anesthesia; iii) pinch reflex, in the absence of deep anesthesia, pinching or clamping the tail of the mouse would result in a flick of the tail and occasional sound. When the tumor volume reached 70-80 mm^3, the mice were randomly divided into two groups: Mock group (n=6) and propofol group (n=6). The propofol group was intraperitoneally injected with 100 mg/kg propofol (Sigma-Aldrich; Merck KGaA) every day for 28 days, and the Mock group was intraperitoneally injected with an equal volume of saline (30). No side effects were observed after relevant administration. The tumor volume was examined every 4 days and calculated with the following formula: (Length x $width^2$)/2. After 28 days, the mice were euthanized by cervical dislocation, and the tumor tissues were collected and weighed. Approval was obtained from the Ethics Committee of Animal Research of the Third Affiliated Hospital of Sun Yat-Sen University.

Reverse transcription-quantitative PCR (RT-qPCR). After relevant transfection and treatment, total RNA was isolated from Hep3B and Huh-7 cells using TRIzol® reagent (cat. no. R0016; Beyotime Institute of Biotechnology). The concentrations and quality of RNAs were examined using NanoDrop 2000c spectrophotometer (Thermo Fisher Scientific, Inc.). For RNA extracted from Hep3B cells, the concentration was 324 ng/μl (OD260/OD280=1.86; OD260/OD230=2.26). For RNA extracted from Huh-7 cells, the concentration was 258 ng/μl (OD260/OD280=1.94; OD260/OD230=2.19). The RT experiment was performed using PrimeScript™ RT reagent kit (cat. no. 6215A; Takara Biotechnology Co., Ltd.) or miRNA 1st Strand cDNA Synthesis kit (cat. no. MR101-01/02; Vazyme Biotech Co., Ltd.) under the conditions of 50˚C for 15 min followed by 85˚C for 5 sec. Then, RT-qPCR was conducted using BeyoFast™ SYBR Green qPCR Mix (cat. no. D7260; Beyotime Institute of Biotechnology) on the ABI 7500 RT PCR system (cat. no. 4351104; Applied Biosystems; Thermo Fisher Scientific, Inc.). The thermocycling conditions of qPCR reaction were: Initial denaturation at 95˚C for 5 min, followed by 40 cycles of 95˚C for 30 sec and 60˚C for 45 sec. The expression levels of HOXA11-AS and miR-4458 were measured using the $2^{-\Delta\Delta Cq}$ method (31). GAPDH or small nuclear RNA U6 were used as an internal reference. The primers were: HOXA11-AS forward (F), 5'-GAGTGTTGG CCTGTCCTC-3' and reverse (R), 5'-TTGTGCCCAGTTGCC TGTAT-3'; miR-4458 F, 5'-AGAGGTAGGTGTGGAAGAA-3' and R, 5'-GCGAGCACAGAATTAATACGAC-3'; GAPDH F, 5'-CGAGCCACATCGCTCAGACA-3' and R, 5'-GTGGTG AAGACGCCAGTGGA-3'; and U6 F, 5'-AGAGCCTGTGGT GTCCG-3' and R, 5'-CATCTTCAAAGCACTTCCCT-3'.

Dual-luciferase reporter assay. The potential target of HOXA11-AS was predicted using software starBase 2. 0 (Sun Yat-sen University) The fragments of HOXA11-AS containing the predicated wild-type (WT) or mutant (MUT) complementary sequences of miR-4458 were amplified and cloned into pmirGLO plasmids (cat. no. E1330; Promega Corporation) to construct luciferase reporter vectors HOXA11-AS WT and HOXA11-AS MUT, respectively. HCC cells ($2x10^4$) were seeded in 24-well plates and 100 ng indicated vector was transfected into HCC cells in combination with 50 nM miR-4458 or miR-NC using Lipofectamine® 2000 (cat. no. 11668-109; Invitrogen; Thermo Fisher Scientific, Inc.). After co-transfection for 48 h, a dual-luciferase reporter assay kit (cat. no. DL101-01; Vazyme Biotech Co., Ltd.) was used to determine luciferase activity. Renilla luciferase activity was normalized to Firefly luciferase activity.

RNA pull-down assay. The Pierce Magnetic RNA-protein pull-down kit (cat. no. 20164; Thermo Fisher Scientific, Inc.) was used to conduct RNA pull-down assay according to the manufacturer's instructions. Then, 50 μM biotinylated miR-4458 (Bio-miR-4458) or its control (Bio-NC) containing putative binding sites of HOXA11-AS were transfected into HCC cells using Lipofectamine® 2000 (cat. no. 11668-109;

Invitrogen; Thermo Fisher Scientific, Inc.). After 24 h, these cells ($1x10^6$ cells) were incubated with streptavidin-coated magnetic beads (Invitrogen; Thermo Fisher Scientific, Inc.) for 2 h at room temperature. Bound RNAs were isolated using TRIzol® reagent after biotin-coupled RNA complex was pulled down. The enrichment of HOXA11-AS was determined via RT-qPCR as aforementioned.

Statistical analysis. The experiments in this study were performed three times and all data are presented as the mean ± SD. Data analysis was performed using GraphPad Prism 7 software (GraphPad Software, Inc.). Unpaired Student's t-test or one-way ANOVA followed by Tukey's test were used to analyze the data. $P<0.05$ was considered to indicate a significantly significant difference.

Results

Propofol suppresses HCC cell proliferation, migration and invasion, and promotes apoptosis in vitro, as well as inhibits tumor growth in vivo. To identify the function of propofol in HCC *in vitro*, Hep3B cells and Huh-7 cells were untreated or treated with different concentrations of propofol (2.5, 5 or 10 μg/ml) and then an MTT assay was conducted. The proliferation of Hep3B and Huh-7 cells was significantly inhibited by propofol in a dose-dependent manner (Fig. 1A and B). It was also found that cell proliferation was ~80% of that in the control group after 5 μg/ml propofol treatment. Thus, 5 μg/ml propofol was selected to treated Hep3B and Huh-7 cells in subsequent experiments.

The results of flow cytometry analysis indicated that cell apoptosis was significantly promoted by propofol treatment in Hep3B and Huh-7 cells (Fig. 1C). Moreover, the expression levels of apoptotic-related proteins Bcl-2 and c-caspase 3 were determined using western blotting. It was demonstrated that Bcl-2 expression was significantly decreased, while c-caspase 3 expression was increased significantly after propofol treatment in both Hep3B and Huh-7 cells (Fig. 1D). Propofol treatment also significantly suppressed the migration and invasion of Hep3B and Huh-7 cells, as identified by the Transwell assay (Fig. 1E-G).

Then, the effect of propofol was evaluated *in vivo*. After propofol treatment, tumor volume was significantly decreased; in Mock group, the diameter ranged between 1.17-1.44 and the volume ranged between 682.3-1,274.9 mm^3, while in propofol group, the diameter ranged between 0.71-1.12 cm and the volume was 174.0-584.1 mm^3 (Fig. 1H). The mice were euthanized after Hep3B cells were injected for 28 days and tumor weight was measured. The results suggested that the tumor weight was significantly reduced after propofol treatment, compared with the Mock group (Fig. 1I). Collectively, these findings indicated that propofol treatment inhibited HCC cell progression *in vitro* and tumor growth *in vivo*.

Propofol treatment significant decreases HOXA11-AS expression in HCC cells. To assess the potential mechanism of propofol on the features of HCC cells, Hep3B and Huh-7 cells were untreated or treated with different doses of propofol (2.5, 5 or 10 μg/ml) for 24 h. It was identified that the expression of HOXA11-AS was significantly decreased after propofol treatment in a concentration-dependent manner in both Hep3B and Huh-7 cells compared with untreated cells (Fig. 2A and B). Thus, it was speculated that propofol may restrain cell proliferation, migration and invasion, as well as induce cell apoptosis via the downregulation of HOXA11-AS in HCC.

HOXA11-AS overexpression weakens the effects on cell proliferation, apoptosis, migration and invasion mediated by propofol in HCC. It was demonstrated that HOXA11-AS transfection resulted in a significantly elevation in HOXA11-AS expression in both Hep3B and Huh-7 cells (Fig. S1A). Next, to investigate whether propofol could regulate the features of HCC cells by downregulating HOXA11-AS, Hep3B and Huh-7 cells were untreated or treated with propofol, propofol + Vector or propofol + HOXA11-AS. RT-qPCR results suggested that the reduction of HOXA11-AS expression caused by propofol was partially reversed after HOXA11-AS overexpression in both Hep3B and Huh-7 cells (Fig. 3A).

MTT assay results indicated that cell proliferation was significantly suppressed by propofol treatment, but this effect was partly reversed by HOXA11-AS transfection in Hep3B and Huh-7 cells (Fig. 3B and C). Moreover, as indicated by flow cytometry analysis, the promotional effect on cell apoptosis mediated by propofol was partially abolished by HOXA11-AS transfection in Hep3B and Huh-7 cells (Figs. 3D and S2A). It was also demonstrated that the protein expression levels of PCNA, cyclinD1, c-Myc and Bcl-2 were significantly reduced, while the protein expression levels of Bax, c-caspase 3 and c-PARP were significantly elevated by propofol in Hep3B and Huh-7 cells; however, these effects were all reversed by HOXA11-AS transfection (Fig. 3E-H). The inhibitory effects of propofol treatment on cell migration and invasion were also partly abrogated after the overexpression of HOXA11-AS in Hep3B and Huh-7 cells, as indicated by Transwell assay (Figs. 3I and J, S2B and C). Moreover, it was found that propofol treatment increased E-cadherin expression and decreased N-cadherin and Vimentin expression levels in Hep3B and Huh-7 cells, while the effects were reversed by HOXA11-AS (Fig. 3K and L). Therefore, these results suggested that propofol suppressed cell progression and metastasis by downregulating HOXA11-AS in HCC cells.

HOXA11-AS negatively regulates the expression of miR-4458 via direct interaction in HCC cells. By searching the online software starBase 2.0, it was found that miR-4458 was a target of HOXA11-AS, and their complementary binding sites are presented in Fig. 4A. RT-qPCR assay results demonstrated that miR-4458 transfected led to a significant elevation in miR-4458 expression in Hep3B and Huh-7 cells, indicating the successful transfection of miR-4458 (Fig. S1C). To assess this prediction, a dual-luciferase reporter assay was conducted. The results suggested that the luciferase activity was significantly suppressed in HOXA11-AS WT + miR-4458 co-transfected Hep3B and Huh-7 cells compared with HOXA11-AS WT + miR-NC co-transfected cells, while co-transfection of HOXA11-AS MUT + miR-4458 or miR-NC did not affect the luciferase activity (Fig. 4B and C). RNA pull-down assay identified that Bio-miR-4458 pulled down HOXA11-AS to a greater extent compared with Bio-NC in Hep3B and Huh-7 cells, which further support the prediction interaction (Fig. 4D).

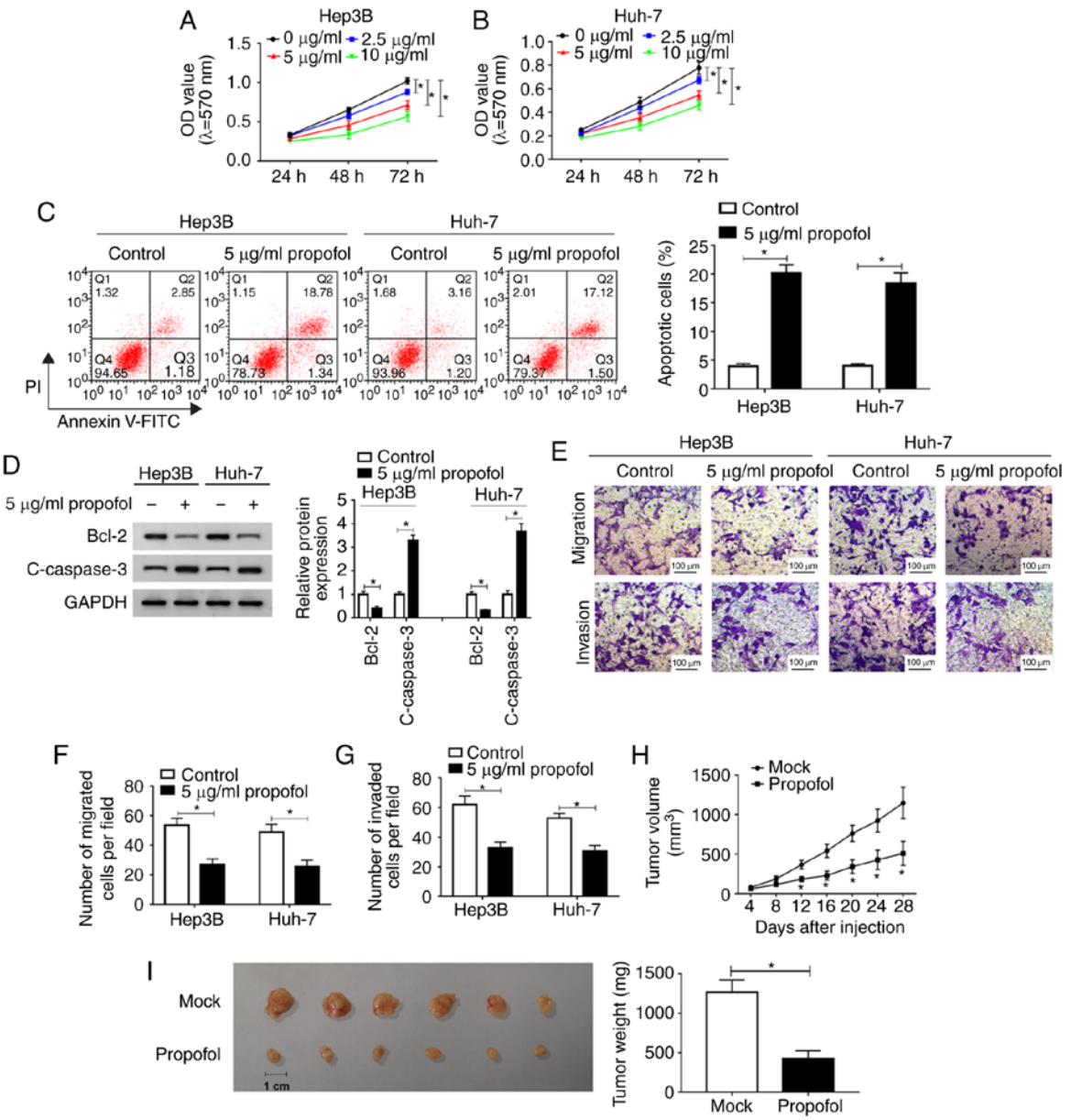

Figure 1. Propofol inhibits HCC cell proliferation, migration and invasion, and induces cell apoptosis *in vitro*, as well as represses tumor growth *in vivo*. Cell proliferation in (A) Hep3B and (B) Huh-7 cells untreated or treated with different concentrations of propofol (2.5, 5 or 10 μg/ml) was measured using a MTT assay. (C) Cell apoptosis in Hep3B and Huh-7 cells treated with 5 μg/ml propofol was analyzed via flow cytometry analysis. (D) Protein expression levels of Bcl-2 and c-caspase 3 in Hep3B and Huh-7 cells treated with 5 μg/ml propofol were examined using western blotting. (E) Migration was (F) determined, along with (G) invasion in Hep3B and Huh-7 cells treated with 5 μg/ml propofol using a Transwell assay. Scale bar, 100 μm. (H) Tumor volume was detected every 4 days after Hep3B cells were injected into the mice. (I) Tumor weight was measured after the mice were euthanized. Experiments were repeated three times. *P<0.05 vs. Mock. PI, propidium iodide; OD, optical density; c- cleaved.

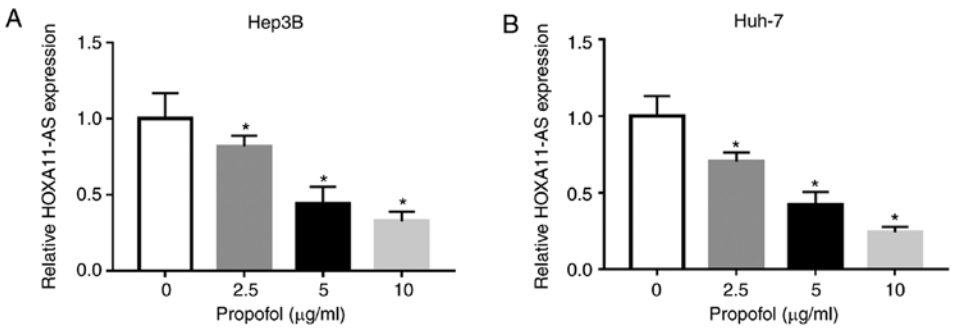

Figure 2. HOXA11-AS is downregulated in HCC cells treated with propofol. Expression of HOXA11-AS in (A) Hep3B and (B) Huh-7 cells untreated or treated with 2.5, 5 or 10 μg/ml propofol for 24 h was determined using reverse transcription-quantitative PCR. Experiments were repeated three times. *P<0.05 vs. 0 μg/ml. HOXA11-AS, HOMEOBOX A11 antisense RNA.

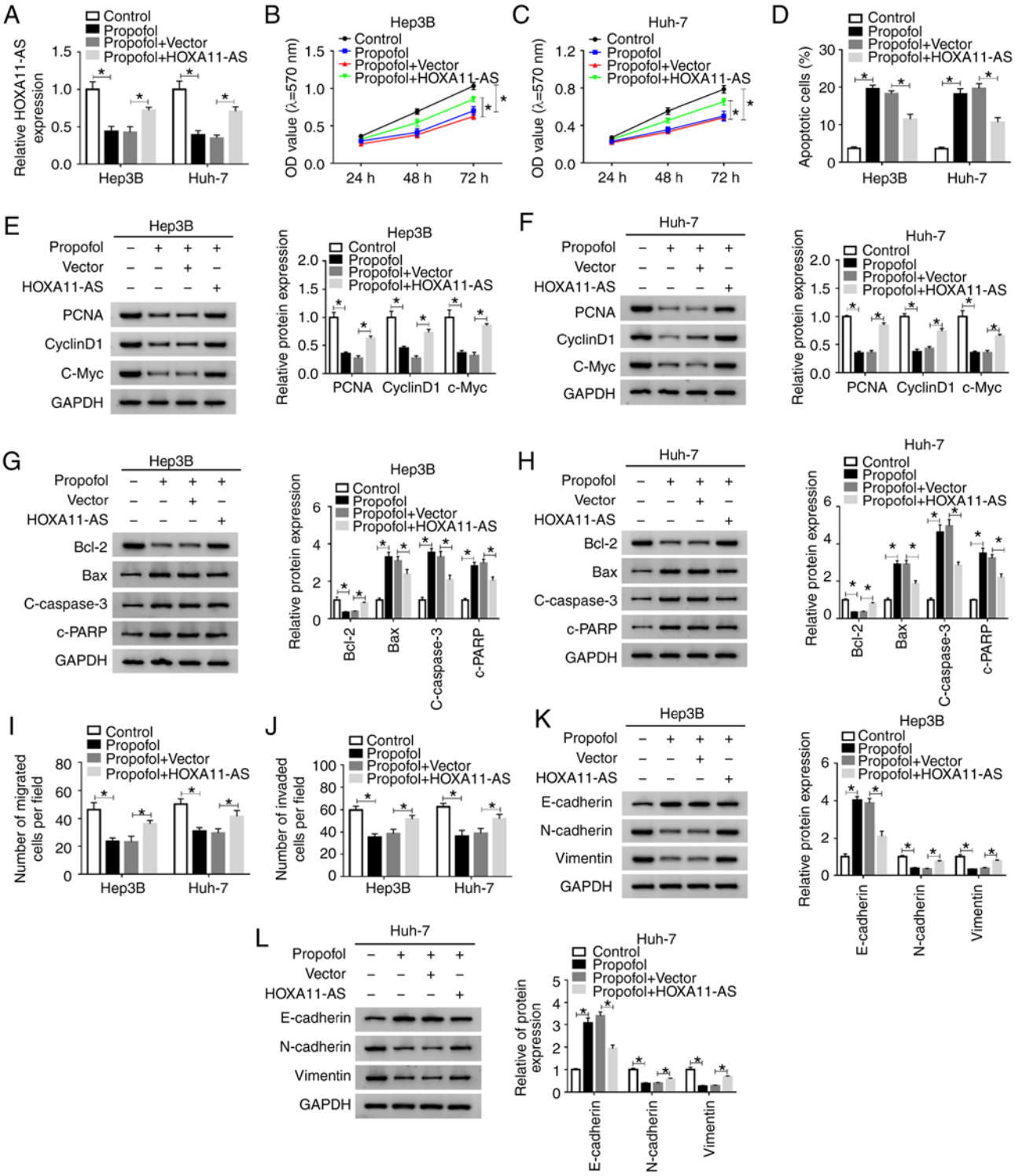

Figure 3. HOXA11-AS restores the effects of propofol on cell proliferation, apoptosis, migration and invasion in HCC. Hep3B and Huh-7 cells were untreated or treated with propofol, propofol + Vector or propofol + HOXA11-AS. (A) Expression of HOXA11-AS in Hep3B and Huh-7 cells was determined using reverse transcription-quantitative PCR. Proliferation of (B) Hep3B and (C) Huh-7 cells was evaluated using MTT assay. (D) Apoptosis of Hep3B and Huh-7 cells was analyzed via flow cytometry analysis. Protein expression levels of PCNA, cyclinD1 and C-Myc in (E) Hep3B and (F) Huh-7 cells were analyzed using western blotting. Protein expression levels of Bcl-2, Bax, c-caspase3 and c-PRRP in (G) Hep3B and (H) Huh-7 cells were analyzed using western blotting. (I) Migration and (J) invasion of Hep3B and Huh-7 cells were assessed using Transwell assay. Protein expression levels of E-cadherin, N-cadherin and Vimentin in (K) Hep3B and (L) Huh-7 cells were analyzed using western blotting. Experiments were repeated three times. *P<0.05. HOXA11-AS, HOMEOBOX A11 antisense RNA; c-, cleaved; PCNA, proliferating cell nuclear antigen; PARP, poly(ADP-ribose) polymerase 1.

Subsequently, three HOXA11-AS knockdown vectors (si-HOXA11-AS#1, si-HOXA11-AS#2 and si-HOXA11-AS#3) were constructed and then transfected into Hep3B and Huh-7 cells. RT-qPCR was performed to evaluate the knockdown efficiency. The data suggested that HOXA11-AS was significantly downregulated after HOXA11-AS knockdown vectors were transfected in Hep3B and Huh-7 cells compared with si-NC groups; si-HOXA11-AS#1 was selected for the

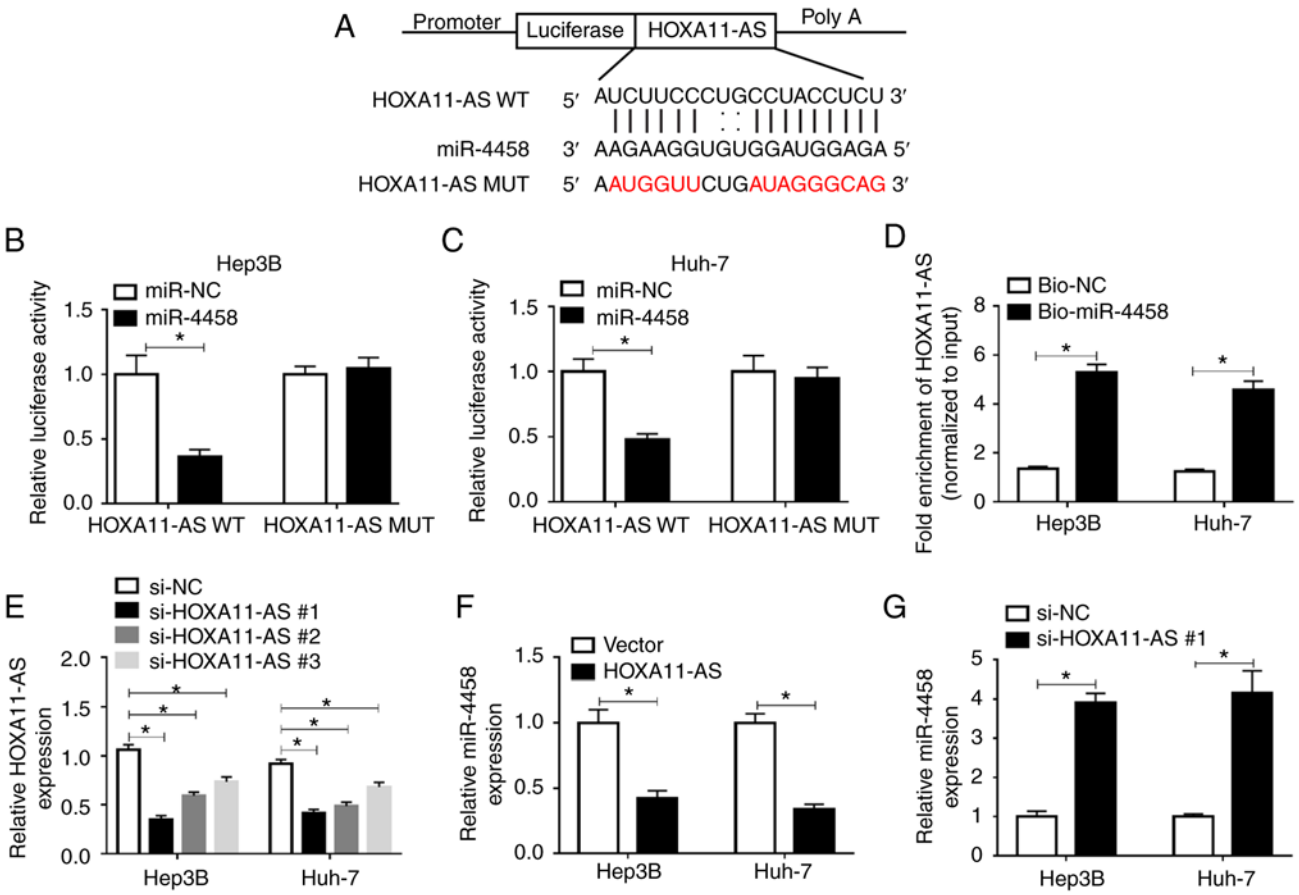

Figure 4. HOXA11-AS negatively regulates miR-4458 expression via direct targeting in HCC cells. (A) Putative binding sites between HOXA11-AS and miR-4458 were predicted using starBase 2.0. Luciferase activity in HOXA11-AS WT or HOXA11-AS MUT and miR-4458 or miR-NC co-transfected (B) Hep3B and (C) Huh-7 cells was detected via dual-luciferase reporter assay. (D) RNA pull-down assay was conducted to assess the interaction between HOXA11-AS and miR-4458, and the expression of HOXA11-AS was detected using RT-qPCR after Bio-miR-4458 or Bio-NC was transfected into Hep3B and Huh-7 cells. (E) Expression of HOXA11-AS in Hep3B and Huh-7 cells transfected with si-NC, si-HOXA11-AS#1, si-HOXA11-AS#2 or si-HOXA11-AS#3 was determined via RT-qPCR. (F) Expression of miR-4458 in Hep3B and Huh-7 cells transfected with Vector or HOXA11-AS was determined via RT-qPCR. (G) Expression of miR-4458 in Hep3B and Huh-7 cells transfected with si-NC or si-HOXA11-AS#1 was measured using RT-qPCR. Experiments were repeated three times. *P<0.05. HOXA11-AS, HOMEOBOX A11 antisense RNA; NC, negative control; miR, microRNA; WT, wild-type; MUT, mutant; RT-qPCR, reverse transcription-quantitative PCR; bio, Biotinylated; si, small interfering RNA.

subsequent experiments due to its stronger inhibitory effects on HOXA11-AS expression compared with si-HOXA11-AS#2 and si-HOXA11-AS#3 (Fig. 4E). HOXA11-AS overexpression led to a significant reduction in miR-4458 expression, while HOXA11-AS downregulation resulted in a significant elevation in miR-4458 expression in both Hep3B and Huh-7 cells (Fig. 4F and G). Thus, HOXA11-AS could target miR-4458 and negatively regulate miR-4458 expression in HCC cells.

miR-4458 inhibition attenuates the effects of HOXA11-AS knockdown on cell proliferation, apoptosis, migration and invasion in HCC cells. Anti-miR-4458 transfection significantly decreased the expression of miR-4458 in Hep3B and Huh-7 cells (Fig. S1B). Subsequently, in order to identify whether HOXA11-AS could affect cell progression by regulating the expression of miR-4458 in HCC, si-NC, si-HOXA11-AS#1, si-HOXA11-AS#1 + anti-miR-NC or si-HOXA11-AS#1 + anti-miR-4458 were transfected into Hep3B and Huh-7 cells. The transfection efficiency was determined using RT-qPCR, and the results demonstrated that si-HOXA11-AS#1 led to a significant increase in miR-4458 expression, while anti-miR-4458 reversed this effect in Hep3B and Huh-7 cells (Fig. 5A).

MTT assay results indicated that knockdown of HOXA11-AS significantly suppressed cell proliferation, while miR-4458 knockdown reversed this suppression in Hep3B and Huh-7 cells (Fig. 5B and C). Flow cytometry analysis indicated that propofol promoted the apoptosis of Hep3B and Huh-7 cells, while HOXA11-AS overexpression reversed the impact. Moreover, the promotional effect on cell apoptosis caused by si-HOXA11-AS#1 was significantly rescued by anti-miR-4458 in Hep3B and Huh-7 cells (Figs. 5D and S3A). The protein expression levels of PCNA, CyclinD1, c-Myc and Bcl-2 were significantly reduced and the protein expression levels of Bax, c-caspase 3 and c-PARP were significantly elevated by silencing of HOXA11-AS in Hep3B and Huh-7 cells, but these effects were reversed by inhibition of miR-4458 (Fig. 5E-H). The Transwell assay results suggested that propofol treatment repressed the migration and invasion of Hep3B and Huh-7 cells, while the overexpression of HOXA11-AS reversed the effects. Furthermore, the inhibition of cell migration and invasion mediated by si-HOXA11-AS#1 was effectively reversed by anti-miR-4458 in Hep3B and Huh-7 cells (Figs. 5I and J, S3B and C). In addition, it was demonstrated that HOXA11-AS knockdown

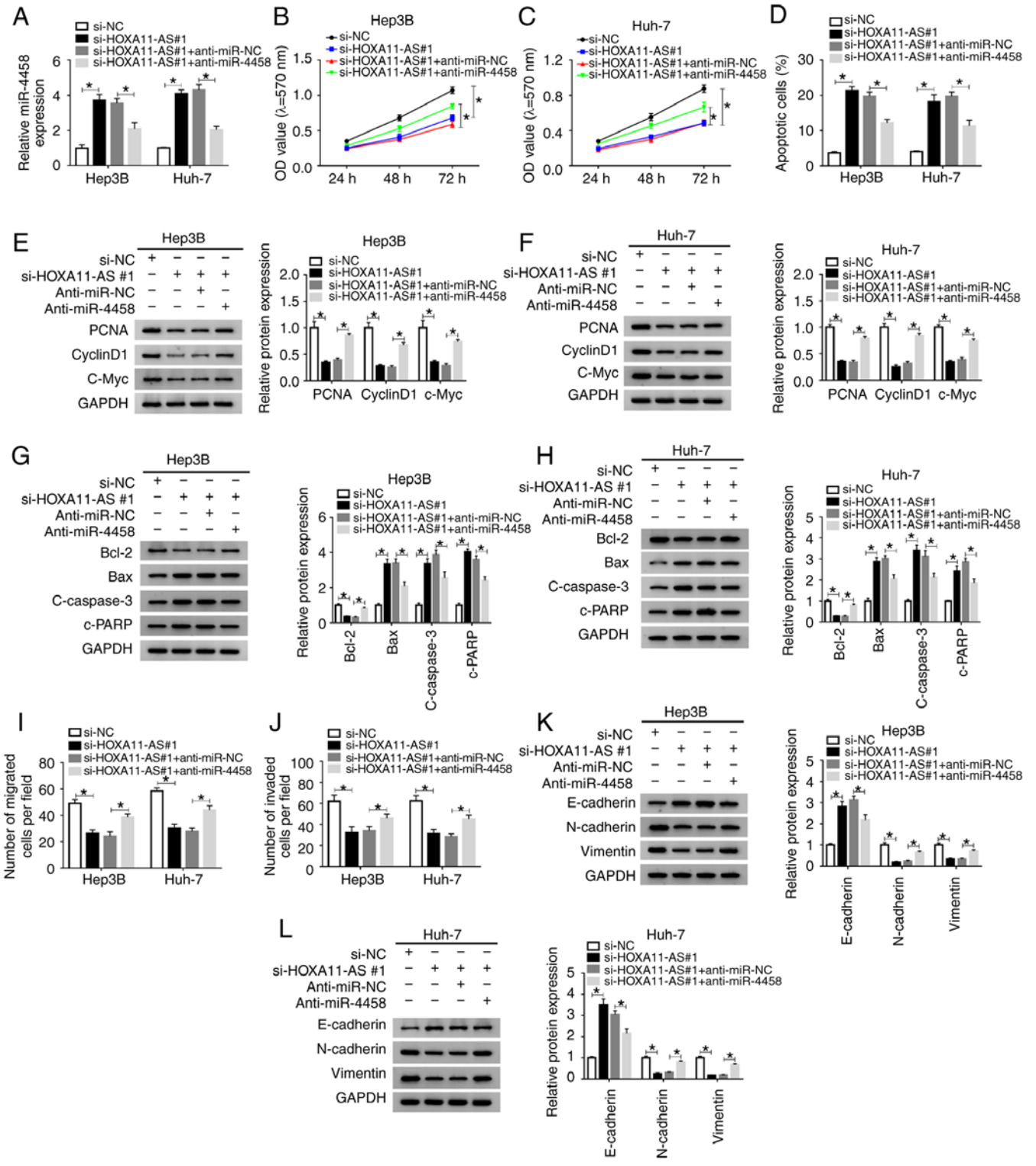

Figure 5. miR-4458 inhibition abolishes the effects of HOXA11-AS knockdown on cell progression in HCC cells. Hep3B and Huh-7 cells were transfected with si-NC, si-HOXA11-AS#1, si-HOXA11-AS#1+anti-miR-NC or si-HOXA11-AS#1+anti-miR-4458. (A) Expression of miR-4458 in Hep3B and Huh-7 cells was measured using reverse transcription-quantitative PCR. Cell proliferation was analyzed by MTT assay in (B) Hep3B and (C) Huh-7 cells. (D) Cell apoptosis was detected via flow cytometry analysis. Protein expression levels of PCNA, cyclinD1 and C-Myc in (E) Hep3B and (F) Huh-7 cells were analyzed using western blotting. Protein expression levels of Bcl-2, Bax, c-caspase3 and c-PRRP in (G) Hep3B and (H) Huh-7 cells were analyzed using western blotting. Cell (I) migration and (J) invasion were assessed using Transwell assay. Protein expression levels of E-cadherin, N-cadherin and Vimentin in (K) Hep3B and (L) Huh-7 cells were analyzed using western blotting. Experiments were repeated three times. *P<0.05. HOXA11-AS, HOMEOBOX A11 antisense RNA; NC, negative control; miR, microRNA; si, small interfering RNA; OD, optical density.

increased E-cadherin expression and decreased N-cadherin and Vimentin expression levels in Hep3B and Huh-7 cells compared with si-NC control groups, while miR-4458 inhibition restored the impacts (Fig. 5K and L). These data indicated that HOXA11-AS regulated cell progression by targeting miR-4458 in HCC cells.

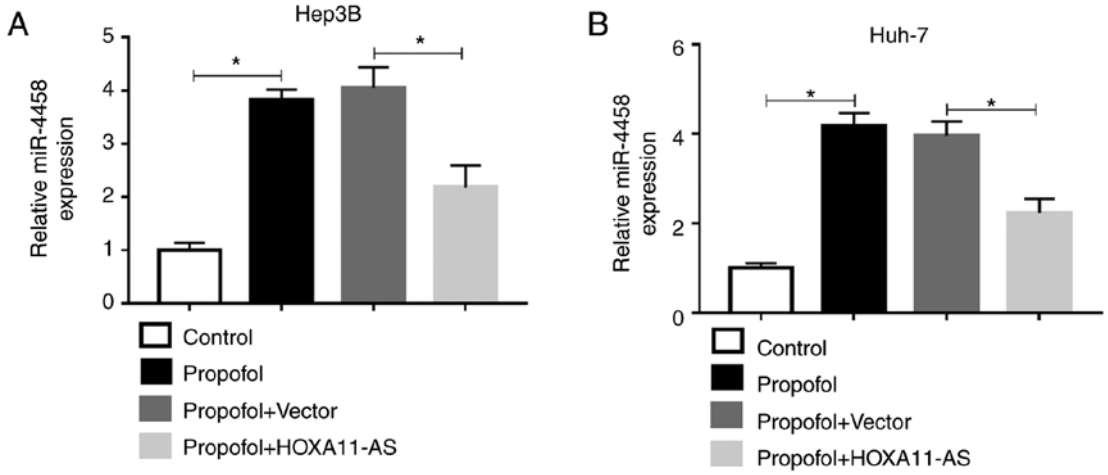

Figure 6. HOXA11-AS abolishes the promotional effect of propofol on the expression of miR-4458 in HCC cells. Expression of miR-4458 in (A) Hep3B and (B) Huh-7 cells untreated or treated with propofol, propofol + Vector or propofol + HOXA11-AS was determined via reverse transcription-quantitative PCR. Experiments were repeated three times. *P<0.05. HOXA11-AS, HOMEOBOX A11 antisense RNA.

HOXA11-AS reverses the upregulation of miR-4458 caused by propofol in HCC cells. To investigate the effect of propofol on miR-4458 expression in HCC cells and the relationship between the expression of HOXA11-AS1 and miR-4458 in HCC cells treated with propofol, Hep3B and Huh-7 cells were untreated or treated with propofol, propofol + Vector or propofol + HOXA11-AS. RT-qPCR results demonstrated that the expression of miR-4458 was significantly increased by propofol, while this effect was partly reversed by HOXA11-AS overexpression in Hep3B and Huh-7 cells (Fig. 6A and B). Therefore, these results suggested that propofol could regulate miR-4458 expression via HOXA11-AS in HCC cells.

Discussion

The metastasis and recurrence of cancer types are the most fundamental factors affecting prognosis (32). Numerous studies have reported that propofol affects the metastasis and recurrence of tumors in multiple cancer types, including HCC (14,33). Therefore, investigating the functions of propofol in the proliferation, metastasis and apoptosis of HCC cells is not only of great theoretical significance, but also important with regards to scientific research and clinical application. In the present study, it was found that propofol could suppress cell progression via downregulating HOXA11-AS and upregulating miR-4458 in HCC.

Ou *et al* (14) reported that propofol led to an inhibition in HCC cell proliferation and metastasis and a promotion in HCC cell apoptosis. Furthermore, Zhang *et al* (33) demonstrated that propofol could suppress cell proliferation and induced cell apoptosis in HCC, while Liu *et al* (34) also revealed that propofol suppressed HCC cell proliferation and metastasis, and induced HCC apoptosis. Consistent with these reports, the present results suggested that there were significant suppressive effects on cell proliferation and metastasis, as well as a significant promotional effect on cell apoptosis after propofol treatment *in vitro* in HCC. Moreover, tumor growth was significantly suppressed *in vivo*. Collectively, these findings indicated that propofol has a tumor suppressor effect on HCC.

Reduced expression levels of lncRNAs mediated by propofol have been revealed in human cancer types. For instance, HOXA11-AS expression is reduced by propofol in colorectal cancer (35). Propofol also induces the apoptosis of cervical cancer cells by repressing HOX transcript antisense RNA (36). In addition, Zhan *et al* (22) reported that HOXA11-AS exerted its promotional role in HCC progression by targeting miR-214-3p. Yu *et al* (37) have also shown that HOXA11-AS silencing could repress HCC cell viability and induce apoptosis *in vitro*, as well as inhibit tumor growth *in vivo*. Based on these findings, it was hypothesized that HOXA11-AS expression could be regulated by propofol treatment and that propofol-induced HOXA11-AS could regulate HCC progression. The current results indicated that HOXA11-AS was suppressed by propofol treatment in a dose-dependent manner. Moreover, HOXA11-AS upregulation reduced the effects of propofol on HCC features, suggesting that HOXA11-AS could promote the development of HCC cells; these present study findings were consistent with previous reports.

To the best of our knowledge, the current study was the first to identify miR-4458 as a target of HOXA11-AS in HCC using dual-luciferase reporter and RNA pull-down assays. A previous study showed that miR-4458 was weakly expressed in HCC and its overexpression inhibited HCC cell proliferation and metastasis, as well as contributed to HCC cell apoptosis (26). The present results indicated that the inhibition of miR-4458 significantly attenuated the inhibitory effect of HOXA11-AS knockdown on cell progression in HCC, suggesting that miR-4458 may serve a tumor suppression effect in HCC. Previous studies have reported that several miRNAs are elevated by propofol in HCC, such as miR-219-5p (28), miR-199a (33) and miR-142-3p (38). Moreover, the current study identified that miR-4458 was stimulated by propofol in HCC cells, while HOXA11-AS reversed this effect.

However, the present study had some limitations. For example, it was not verified whether HOXA11-AS regulated tumorigenesis of HCC *in vivo*. Moreover, the potential target genes of miR-4458 should be examined in future experiments.

In conclusion, propofol inhibited cell progression *in vitro* and tumor growth *in vivo* in HCC. Furthermore, propofol affected the features of HCC cells via the HOXA11-AS/miR-4458 axis in HCC. Therefore, this study demonstrated the potential of propofol during the surgery of patients with HCC and may provide a novel insight for HCC treatment in the future.

Acknowledgements

Not applicable.

Funding

No funding was received.

Availability of data and materials

The datasets used and/or analyzed during the current study are available from the corresponding author on reasonable request.

Authors' contributions

FS and YJ conceived and designed the study. JL and YF performed data analyses and interpretation. FS and YF co-wrote the manuscript. All authors have read and approved the final manuscript.

Ethics approval and consent to participate

Ethical approval was obtained from the Ethics Committee of Animal Research of the Third Affiliated Hospital of Sun Yat-Sen University.

Patient consent for publication

Not applicable.

Competing interests

The authors declare that they have no competing interests.

References

1. Bruix J, Sherman M; American Association for the Study of Liver Diseases: Management of hepatocellular carcinoma: An update. Hepatology 53: 1020-1022, 2011.
2. Mittal S and El-Serag HB: Epidemiology of HCC: Consider the population. J Clin Gastroenterol 47: S2-S6, 2013.
3. Bray F, Ferlay J, Soerjomataram I, Siegel RL, Torre LA and Jemal A: Global cancer statistics 2018: GLOBOCAN estimates of incidence and mortality worldwide for 36 cancers in 185 countries. CA Cancer J Clin 68: 394-424, 2018.
4. Cidon EU: Systemic treatment of hepatocellular carcinoma: Past, present and future. World J Hepatol 9: 797-807, 2017.
5. Yu JJ, Xiao W, Dong SL, Liang HF, Zhang ZW, Zhang BX, Huang ZY, Chen YF, Zhang WG, Luo HP, *et al*: Effect of surgical liver resection on circulating tumor cells in patients with hepatocellular carcinoma. BMC Cancer 18: 835, 2018.
6. Suh SW and Choi YS: Influence of liver fibrosis on prognosis after surgical resection for resectable single hepatocellular carcinoma. ANZ J Surg 89: 211-215, 2019.
7. Ye Z, Jingzhong L, Yangbo L, Lei C and Jiandong Y: Propofol inhibits proliferation and invasion of osteosarcoma cells by regulation of microRNA-143 expression. Oncol Res 21: 201-207, 2013.
8. Huang X, Teng Y, Yang H and Ma J: Propofol inhibits invasion and growth of ovarian cancer cells via regulating miR-9/NF-kappaB signal. Braz J Med Biol Res 49: e5717, 2016.
9. Meng C, Song L, Wang J, Li D, Liu Y and Cui X: Propofol induces proliferation partially via downregulation of p53 protein and promotes migration via activation of the nrf2 pathway in human breast cancer cell line MDA-MB-231. Oncol Rep 37: 841-848, 2017.
10. Chidambaran V, Costandi A and D'Mello A: Propofol: A review of its role in pediatric anesthesia and sedation. CNS Drugs 29: 543-563, 2015.
11. Zhang L, Wang N, Zhou S, Ye W, Jing G and Zhang M: Propofol induces proliferation and invasion of gallbladder cancer cells through activation of Nrf2. J Exp Clin Cancer Res 31: 66, 2012.
12. Wang XY, Li YL, Wang HY, Zhu M, Guo D, Wang GL, Gao YT, Yang Z, Li T, Yang CY and Chen YM: Propofol inhibits invasion and proliferation of C6 glioma cells by regulating the Ca^{2+} permeable AMPA receptor-system xc- pathway. Toxicol *In Vitro* 44: 57-65, 2017.
13. Liu Z, Zhang J, Hong G, Quan J, Zhang L and Yu M: Propofol inhibits growth and invasion of pancreatic cancer cells through regulation of the miR-21/slug signaling pathway. Am J Transl Res 8: 4120-4133, 2016.
14. Ou W, Lv J, Zou X, Yao Y, Wu J, Yang J, Wang Z and Ma Y: Propofol inhibits hepatocellular carcinoma growth and invasion through the HMGA2-mediated wnt/β-catenin pathway. Exp Ther Med 13: 2501-2506, 2017.
15. Fatica A and Bozzoni I: Long non-coding RNAs: New players in cell differentiation and development. Nat Rev Genet 15: 7-21, 2014.
16. Ponting CP, Oliver PL and Reik W: Evolution and functions of long noncoding RNAs. Cell 136: 629-641, 2009.
17. Chen F, Li M and Zhu X: Propofol suppresses proliferation and migration of papillary thyroid cancer cells by down-regulation of lncRNA ANRIL. Exp Mol Pathol 107: 68-76, 2019.
18. Ming N, Na HST, He JL, Meng QT and Xia ZY: Propofol alleviates oxidative stress via upregulating lncRNA-TUG1/Brg1 pathway in hypoxia/reoxygenation hepatic cells. J Biochem 166: 415-421, 2019.
19. Sun Y and Sun H: Propofol exerts anticancer activity on hepatocellular carcinoma cells by raising lncRNA DGCR5. J Cell Physiol 235: 2963-2972, 2019.
20. Xu X, Yin Y, Tang J, Xie Y, Han Z, Zhang X, Liu Q, Qin X, Huang X and Sun B: Long non-coding RNA myd88 promotes growth and metastasis in hepatocellular carcinoma via regulating myd88 expression through H3K27 modification. Cell Death Dis 8: e3124, 2017.
21. Yang Y, Chen Q, Piao HY, Wang B, Zhu GQ, Chen EB, Xiao K, Zhou ZJ, Shi GM, Shi YH, *et al*: HNRNPAB-regulated lncRNA-ELF209 inhibits the malignancy of hepatocellular carcinoma. Int J Cancer 146: 169-180, 2019.
22. Zhan M, He K, Xiao J, Liu F, Wang H, Xia Z, Duan X, Huang R, Li Y, He X, *et al*: Lnc RNA HOXA 11-AS promotes hepatocellular carcinoma progression by repressing miR-214-3p. J Cell Mol Med 22: 3758-3767, 2018.
23. Borel F, Konstantinova P and Jansen PL: Diagnostic and therapeutic potential of miRNA signatures in patients with hepatocellular carcinoma. J Hepatol 56: 1371-1383, 2012.
24. Wang Y, Yang L, Chen T, Liu X, Guo Y, Zhu Q, Tong X, Yang W, Xu Q, Huang D and Tu K: A novel lncRNA MCM3AP-AS1 promotes the growth of hepatocellular carcinoma by targeting miR-194-5p/FOXA1 axis. Mol Cancer 18: 28, 2019.
25. Kabir TD, Ganda C, Brown RM, Beveridge DJ, Richardson KL, Chaturvedi V, Candy P, Epis M, Wintle L, Kalinowski F, *et al*: A microRNA-7/growth arrest specific 6/TYRO3 axis regulates the growth and invasiveness of sorafenib-resistant cells in human hepatocellular carcinoma. Hepatology 67: 216-231, 2018.
26. Tang D, Sun B, Yu H, Yang Z and Zhu L: Tumor-suppressing effect of miR-4458 on human hepatocellular carcinoma. Cell Physiol Biochem 35: 1797-1807, 2015.
27. Wang P, Ning S, Zhang Y, Li R, Ye J, Zhao Z, Zhi H, Wang T, Guo Z and Li X: Identification of lncRNA-associated competing triplets reveals global patterns and prognostic markers for cancer. Nucleic Acids Res 43: 3478-3489, 2015.
28. Gong T, Ning X, Deng Z, Liu M, Zhou B, Chen X, Huang S, Xu Y, Chen Z and Luo R: Propofol-induced miR-219-5p inhibits growth and invasion of hepatocellular carcinoma through suppression of GPC3-mediated wnt/β-catenin signalling activation. J Cell Biochem 120: 16934-16945, 2019.

29. Xu J, Xu W and Zhu J: Propofol suppresses proliferation and invasion of glioma cells by upregulating microRNA-218 expression. Mol Med Rep 12: 4815-4820, 2015.
30. Liu Y, Zhang N, Cao Q, Cui X, Zhou Q and Yang C: The effects of propofol on the growth behavior of hepatoma xenografts in balb/c mice. Biomed Pharmacother 90: 47-52, 2017.
31. Livak KJ and Schmittgen TD: Analysis of relative gene expression data using real-time quantitative PCR and the 2(-Delta Delta C(T)) method. Methods 25: 402-408, 2001.
32. Jiang WG, Sanders AJ, Katoh M, Ungefroren H, Gieseler F, Prince M, Thompson SK, Zollo M, Spano D, Dhawan P, *et al*: Tissue invasion and metastasis: Molecular, biological and clinical perspectives. Semin Cancer Biol 35: S244-S275, 2015.
33. Zhang J, Wu Gq, Zhang Y, Feng Zy and Zhu Sm: Propofol induces apoptosis of hepatocellular carcinoma cells by upregulation of microRNA-199a expression. Cell Biol Int 37: 227-232, 2013.
34. Liu SQ, Zhang JL, Li ZW, Hu ZH, Liu Z and Li Y: Propofol inhibits proliferation, migration, invasion and promotes apoptosis through down-regulating miR-374a in hepatocarcinoma cell lines. Cell Physiol Biochem 49: 2099-2110, 2018.
35. Ren YL and Zhang W: Propofol promotes apoptosis of colorectal cancer cells via alleviating the suppression of lncRNA HOXA11-AS on miRNA let-7i. Biochem Cell Biol 98: 90-98, 2019.
36. Zhang D, Zhou XH, Zhang J, Zhou YX, Ying J, Wu GQ and Qian JH: Propofol promotes cell apoptosis via inhibiting HOTAIR mediated mTOR pathway in cervical cancer. Biochem Biophys Res Commun 468: 561-567, 2015.
37. Yu J, Hong JF, Kang J, Liao LH and Li CD: Promotion of LncRNA HOXA11-AS on the proliferation of hepatocellular carcinoma by regulating the expression of LATS1. Eur Rev Med Pharmacol Sci 21: 3402-3411, 2017.
38. Zhang J, Shan Wf, Jin Tt, Wu GQ, Xiong XX, Jin Hy and Zhu Sm: Propofol exerts anti-hepatocellular carcinoma by microvesicle-mediated transfer of miR-142-3p from macrophage to cancer cells. J Transl Med 12: 279, 2014.